

# Bilateral Boundary Control of Moving Shockwave in LWR Model of Congested Traffic

Huan Yu, *Student Member, IEEE*, Mamadou Diagne, *Member, IEEE*, Liguozhang *Member, IEEE*,  
Miroslav Krstic, *Fellow, IEEE*

**Abstract**—We develop backstepping state feedback control to stabilize a moving shockwave in a freeway segment under bilateral boundary actuations of traffic flow. A moving shockwave, consisting of light traffic upstream of the shockwave and heavy traffic downstream, is usually caused by changes of local road situations. The density discontinuity travels upstream and drivers caught in the shockwave experience transitions from free to congested traffic. Boundary control design in this paper brings the moving shockwave front to a static setpoint position, hindering the upstream propagation of traffic congestion. The traffic dynamics are described with Lighthill-Whitham-Richard (LWR) model, leading to a system of two first-order hyperbolic partial differential equations (PDEs). Each represents the traffic density of a spatial domain segregated by the moving interface. By Rankine-Hugoniot condition, the interface position is driven by flux discontinuity and thus governed by a PDE state dependent ordinary differential equation (ODE). For the PDE-ODE coupled system, the control objective is to stabilize both the PDE states of traffic density and the ODE state of moving shock position to setpoint values. Using delay representation and backstepping method, we design predictor feedback controllers to cooperatively compensate state-dependent input delays to the ODE. From Lyapunov stability analysis, we show local stability of the closed-loop system in  $H^1$  norm. The performance of controllers is demonstrated by numerical simulation.

**Index Terms**—Backstepping control, State-dependent delay compensation, PDE-ODE coupled system, Moving shockwave, LWR traffic model

## I. INTRODUCTION

Consider a common phenomenon in freeway traffic when there is a moving shockwave consisting of light traffic upstream of the shockwave and heavy traffic downstream. The shockwave conserves traffic flow at the interface of discontinuity and is caused by local changes of road situations like uphill and downhill gradients, curves, change of speed limits. The upstream propagation of the moving shockwave causes more and more vehicles entering into the congested traffic. The abrupt transition from free to congested traffic at the moving interface leads to unsafe driving conditions and increased fuel consumptions. It is of great importance if we can halt the upstream propagation and drive the moving interface to a desirable location where the traffic congestion could be

discharged by traffic management infrastructures on freeways. Ramp metering and varying speed limit are most widely used to control traffic flux or velocity from the boundary of a stretch of freeway so that desirable traffic states could be achieved for the inner domain of the freeway segment.

In developing boundary control strategies through ramp metering and varying speed limit, many recent efforts [5],[12],[20],[21],[22],[23],[24],[25] are focused on macroscopic traffic models governed by PDE system. These model-based controllers regulate the evolution of traffic densities and velocities in order to dissipate traffic congestions on freeways. For instance, [20],[21] achieve  $L^2$  norm stabilization of stop-and-go traffic by nonlinear second-order PDE traffic model using boundary control.

Traffic discontinuity can be caused by various inhomogeneities of freeway or vehicles. Some studies consider it as a moving traffic flux constraint [9],[18] due to a reduction of road capacity. Slow moving vehicles, also known as moving bottlenecks, are represented in [6],[15],[24] with ODEs governing the velocity of slow vehicles. These are out of the scope of this paper and relevant to the controllability problem with boundary actuation. In this paper, we consider the situation where road capacity is conserved but shockwaves form due to uphill, downhill, and curves of the road. Higher density traffic appears downstream of the shockwave front and the front of density discontinuity keeps moving upstream, driven by the flux discontinuity. The upstream propagation of the moving shockwave causes traffic congestion forming up on a freeway.

In this work, we adopt the seminal Lighthill, Whitham and Richards (LWR) model to describe the traffic dynamics of the moving shockwave problem. The LWR model is a first-order, hyperbolic macroscopic PDE model of traffic density. It is simple yet very powerful to describe the formation, dissipation and propagation of traffic shockwaves on a freeway. The moving shockwave consists of upstream, downstream traffic and a moving interface. The upstream and downstream traffic densities are governed by LWR PDE models and the interface position is governed by Rankine-Hugoniot jump condition, leading to a density state-dependent nonlinear ODE. Therefore, we are dealing with a PDE-ODE coupled system, where ODE state is dependent on PDE states at the moving interface. The traffic flow is actuated at both boundaries of a freeway segment and can be realized with ramp-metering. The control objective is to drive the moving interface to certain location and traffic states to steady values through bilateral boundary controls.

Huan Yu and Miroslav Krstic are with the Department of Mechanical and Aerospace Engineering, University of California, San Diego, 9500 Gilman Dr, La Jolla, CA 92093. Email: huy015@ucsd.edu, krstic@ucsd.edu

Mamadou Diagne is with the Department of Mechanical Aerospace and Nuclear Engineering, Rensselaer Polytechnic Institute, New York, 12180, USA. Email: diagnm@rpi.edu

Liguozhang is with the School of Electronic Information and Control Engineering, Beijing University of Technology, Beijing, 100124, China. Email: zhangliguo@bjut.edu.cn

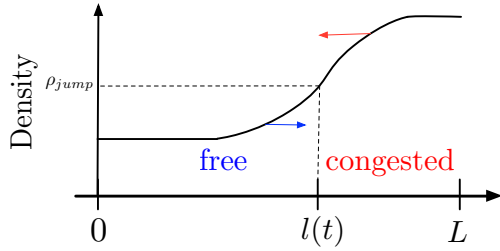


Fig. 1. Traffic moving shockwave front on freeway, the arrows represent propagation directions of density variations. In LWR model, the propagation directions are given by the characteristic speeds of density  $Q'(\rho)$ .

Boundary control of PDE with state-dependent ODE systems has been intensively studied over the past few years. Backstepping control design method is used in solving these problems. In parabolic PDE system, the problem is known as Stefan problem with application to control of screw extruder for 3D Printing [14] and arctic sea ice temperature estimation [13]. In hyperbolic PDE system, theoretical results have been studied by [2],[3],[4],[11],[17]. With application, [7] develops boundary control piston position in inviscid gas and [10] develops the control of a mass balance in screw extrusion process. Other applications include vibration suppression of mining cable elevator [19], control of Saint-Venant equation with hydraulic jumps [1]. However, the application of the methodology in traffic problem has never been discussed before.

The contribution of this paper is twofold. This is the very first theoretical result on control of two PDE state-dependent input delays to ODE. Predictor-based state feedback design approach is adopted following [11],[17]. In fact, [17] shows a predictor feedback design for multiple constant delayed inputs to linear time-invariant systems while [11] considers a single implicitly defined state-dependent input delay to nonlinear time-invariant systems alternatively written as a PDE-ODE cascade system. In this work, we firstly present the predictor feedback design for two PDE states dependent input delays to ODE. On the other hand, control problem of traffic moving shockwave has never been addressed before to author's best knowledge.

The outline of this paper: we introduce the LWR model to describe the moving shockwave problem. Then we linearized the coupled PDE-ODE model around steady states. The predictor state feedback control design follows and using Lyapunov analysis, we prove the local exponential stability of the closed-loop system. Model validity is guaranteed with the control design. In the end, the result is validated with numerical simulations.

## II. PROBLEM STATEMENT

The moving shockwave front is the head of a shockwave, segregating traffic on a segment of freeway into two different schemes. The upstream traffic of the shockwave front is in free regime and the downstream is in congested regime, as shown in Fig.1. The traffic densities are described with the first-order macroscopic LWR model.

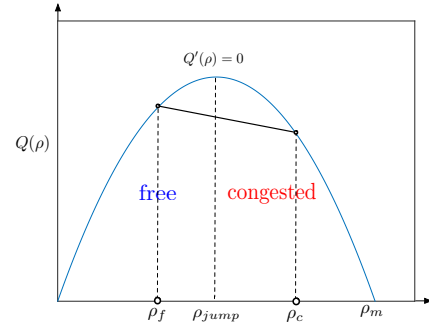


Fig. 2. Fundamental diagram of traffic density and traffic flux relation

### A. LWR traffic model

In LWR model, traffic density  $\rho(x, t)$  is governed by the following first-order nonlinear hyperbolic PDE, where  $x \in [0, L]$ ,  $t \in [0, \infty)$ ,

$$\partial_t \rho + Q'(\rho) \partial_x \rho = 0, \quad (1)$$

where  $Q(\rho)$  is a fundamental diagram which shows the relation of equilibrium density and traffic flux. The fundamental diagram  $Q(\rho)$  is defined as  $Q(\rho) = \rho V(\rho)$ . The equilibrium velocity  $V(\rho)$  is a decreasing function of density. We choose the following Greenshield's model for  $V(\rho)$  in which velocity is a linear decreasing function of density.

$$V(\rho) = v_m \left( 1 - \frac{\rho}{\rho_m} \right). \quad (2)$$

where  $v_m$  is the maximum speed,  $\rho_m$  is the maximum density. Greenshield's model  $V(\rho)$  yields that the fundamental diagram  $Q(\rho)$  is a quadratic map, shown in figure Fig. 2. The jump density  $\rho_{jump}$  segregates densities into two sections, the density smaller than  $\rho_{jump}$  is defined as free-regime while the density greater than  $\rho_{jump}$  is defined as congested regime.

In the LWR PDE (1), density variations propagate with the characteristic speed  $Q'(\rho)$ . The free regime with light traffic, equivalently,  $\rho_f < \rho_{jump}$ , has its density variations transported downstream with

$$Q'(\rho)|_{\rho=\rho_f} = V(\rho_f) + \rho_f V'(\rho_f) > 0, \quad (3)$$

while the congested regime with denser traffic, namely,  $\rho_c > \rho_{jump}$  has its density variations transported upstream with

$$Q'(\rho)|_{\rho=\rho_c} = V(\rho_c) + \rho_c V'(\rho_c) < 0. \quad (4)$$

As shown in figure Fig. 1, the moving shockwave considered here is the shock of a traffic wave which physically represents the discontinuity of density. The congested traffic density propagates upstream while the light traffic density propagates downstream. Therefore, the upstream front of the shockwave becomes steeper in propagation and eventually, the gradient  $\partial_x \rho$  tends to be infinity [16]. In this context, drivers located in the upstream front of the shock will experience transition from free to congested traffic. The position of the shockwave front is later defined by an ODE according to Rankine-Hugoniot condition.

### B. Moving shockwave model

The moving shockwave model consists of upstream, downstream traffic densities and a moving interface located at the density discontinuity spatial coordinate. The dynamics of the upstream free traffic, the downstream congested traffic and the position of the moving interface are presented below, respectively.

Define the traffic density of the congested regime as  $\rho_c(x, t)$  for  $x \in [0, l(t)]$ ,  $t \in [0, +\infty]$ , and the free regime as  $\rho_f(x, t)$ , for  $x \in [l(t), L]$ ,  $t \in [0, +\infty]$ , the LWR model that describes the traffic is given by

$$\partial_t \rho_f + \partial_x (\rho_f v_f) = 0, \quad x \in [0, l(t)] \quad (5)$$

$$\partial_t \rho_c + \partial_x (\rho_c v_c) = 0, \quad x \in [l(t), L] \quad (6)$$

where  $l(t) \in [0, L]$  is the location of moving interface. The density and velocity relation is given by Greenshield's model in (2), ( $i = f, c$ ),

$$v_i(x, t) = V_i(\rho_i(x, t)) = v_m \left( 1 - \frac{\rho_i(x, t)}{\rho_m} \right). \quad (7)$$

Due to the flux discontinuity at the moving boundary, a traveling vehicle leaves the free regime to enter the congested regime. Dynamics of moving interface  $l(t)$  is derived under the Rankine-Hugoniot condition which guarantees that the mass of traffic flow is conserved at the moving interface. The upstream propagation of the shockwave front is driven by the flux discontinuity.

$$\dot{l}(t) = \frac{\rho_c(l(t), t) v_c(l(t), t) - \rho_f(l(t), t) v_f(l(t), t)}{\rho_c(l(t), t) - \rho_f(l(t), t)}, \quad (8)$$

where the initial position of the shockwave front  $0 < l(0) < L$ . The following inequalities for initial conditions of PDEs (5),(6) are assumed

$$\rho_c(l(0), 0) v_c(l(0), 0) < \rho_f(l(0), 0) v_f(l(0), 0), \quad (9)$$

$$\rho_c(l(0), 0) > \rho_f(l(0), 0). \quad (10)$$

Initially, the traffic downstream the interface is denser but with a smaller flux which lets less vehicles to pass through while the traffic upstream is light and let more vehicles to come in the segment. With the above assumptions to hold, we obtain from (8) that  $\dot{l}(0) < 0$ . The moving interface is traveling upstream and is driven by a flux difference induced by the density discontinuity.

Substituting density-velocity relation in (7) into (5),(6), and (8), we have two nonlinear PDEs and an ODE coupled system describing the dynamics of  $\rho_f(x, t)$ ,  $\rho_c(x, t)$  and  $l(t)$  given by

$$\partial_t \rho_f(x, t) = -v_m \partial_x \left( \rho_f(x, t) - \frac{\rho_f^2(x, t)}{\rho_m} \right), \quad (11)$$

$$\partial_t \rho_c(x, t) = -v_m \partial_x \left( \rho_c(x, t) - \frac{\rho_c^2(x, t)}{\rho_m} \right), \quad (12)$$

$$\dot{l}(t) = v_m - \frac{v_m}{\rho_m} (\rho_c(l(t), t) + \rho_f(l(t), t)). \quad (13)$$

*Remark 1:* For model validity, we assume that there exists a constant  $L > 0$  such that the ODE state  $l(t)$  satisfies

$$0 < l(t) < L, \quad (14)$$

so that (11),(12), and (13) are well-defined for  $x \in [0, L]$ ,  $t \in [0, +\infty]$ . We emphasize that the proposed control law needs to guarantee the above condition.

Our control objective is to stabilize both free and congested regime traffic  $\rho_i(x, t)$  to uniform steady states  $\rho_i^*$  and at the same time, the moving interface  $l(t)$  to a desirable static setpoint  $l^*$ . Therefore, the shockwave becomes standstill within the freeway segment instead of moving upstream.

We consider the following controlled boundary condition for the nonlinear coupled PDE-ODE system consisting of (11), (12), and (13)

$$\rho_f(0, t) = U_{in}(t) + \rho_f^*, \quad (15)$$

$$\rho_c(L, t) = U_{out}(t) + \rho_c^*, \quad (16)$$

where we control the incoming and outgoing density variations of the freeway segment  $U_{in}(t)$  and  $U_{out}(t)$ . As mentioned in Section I, the control of density can be realized with on-ramp metering actuating the flux at both boundaries:

$$q_{in}(t) = Q(\rho_f(0, t)), \quad (17)$$

$$q_{out}(t) = Q(\rho_c(L, t)). \quad (18)$$

### III. LINEARIZED MODEL

Now, we linearize the coupled PDE-ODE model ( $\rho_f(x, t), \rho_c(x, t), l(t)$ )-system defined in (11),(12) and (13) around steady states and setpoint ( $\rho_f^*, \rho_c^*, l^*$ ). The constant equilibrium setpoint values are chosen so that the following conditions that ensure the model validity hold

$$0 < \rho_f^* < \rho_{jump} < \rho_c^* < \rho_m, \quad (19)$$

$$0 < l^* < L. \quad (20)$$

At steady-state, the flux equilibrium needs to be achieved for both sides of the moving interface. Hence,

$$\rho_f^* V(\rho_f^*) = \rho_c^* V(\rho_c^*). \quad (21)$$

Using condition (21), the quadratic fundamental diagram yields that

$$\rho_f^* + \rho_c^* = \rho_m. \quad (22)$$

Define the state deviations from the system reference as

$$\tilde{\rho}_i(x, t) = \rho_i(x, t) - \rho_i^*, \quad (23)$$

$$X(t) = l(t) - l^*, \quad (24)$$

where  $\dot{X}(t) = \dot{l}(t)$  is satisfied. Thus, the linearized PDE-ODE model (11)-(13) with the boundary conditions (15) and (16) around the system reference ( $\rho_f^*, \rho_c^*, l^*$ ) is defined as the following ( $\tilde{\rho}_f(x, t), \tilde{\rho}_c(x, t), X(t)$ )-system

$$\partial_t \tilde{\rho}_f(x, t) = -u \partial_x \tilde{\rho}_f(x, t), \quad x \in [0, l(t)] \quad (25)$$

$$\partial_t \tilde{\rho}_c(x, t) = u \partial_x \tilde{\rho}_c(x, t), \quad x \in [l(t), L] \quad (26)$$

$$\tilde{\rho}_f(0, t) = U_{in}(t), \quad (27)$$

$$\tilde{\rho}_c(L, t) = U_{out}(t), \quad (28)$$

$$\dot{X}(t) = -b (\tilde{\rho}_f(l(t), t) + \tilde{\rho}_c(l(t), t)), \quad (29)$$

where the transport speed is defined as

$$u = v_m \left( 1 - \frac{2\rho_f^*}{\rho_m} \right), \quad (30)$$

and satisfy  $0 < u < v_m$ . The constant coefficient  $b$  in ODE is defined as  $b = \frac{v_m}{\rho_m} > 0$ . The linearized model (25)-(29) is a PDE-ODE coupled system with bilateral boundary control inputs from inlet and outlet.

#### IV. PREDICTOR-BASED CONTROL DESIGN

In this section, we first introduce the equivalent delay system representation to the system (25)-(29). Then, a backstepping transformation is applied to obtain predictor-based state feedback controls to compensate the PDE state-dependent delays to the ODE.

##### A. From coupled PDE-ODE to delay system representation

The system (25)-(29) can be represented by an unstable ODE with two distinct state-dependent input delays. Introduce the following state-dependent delays for the two transport PDEs

$$D_f(t) = \frac{l(t)}{u}, \quad (31)$$

$$D_c(t) = \frac{L - l(t)}{u}, \quad (32)$$

where  $l(t) = X(t) + l^*$ . The PDE states are represented by

$$\tilde{\rho}_f(l(t), t) = U_{\text{in}}(t - D_f(t)), \quad (33)$$

$$\tilde{\rho}_c(l(t), t) = U_{\text{out}}(t - D_c(t)), \quad (34)$$

where  $U_{\text{in}}(t)$  and  $U_{\text{out}}(t)$  are the boundary control inputs defined in (27) and (28). Substituting (33) and (34) into the ODE (29), the following state-dependent input delay system representation is derived

$$\dot{X}(t) = -b(U_{\text{in}}(t - D_f(X(t))) + U_{\text{out}}(t - D_c(X(t)))) \quad (35)$$

*Remark 2:* If the position of the moving shock front is close to the inlet half segment such that  $l(t) \in [0, \frac{L}{2}]$ , it holds that  $\forall t \in [0, \infty), D_f(t) \leq D_c(t)$ . As a result, delayed inlet control input  $U_{\text{in}}(t - D_f(t))$  reaches the moving shock front faster than delayed outlet control input  $U_{\text{out}}(t - D_c(t))$ . If  $l(t) \in [\frac{L}{2}, L]$ ,  $\forall t \in [0, \infty), D_f(t) \geq D_c(t)$  holds. Then  $U_{\text{out}}(t - D_c(t))$  reaches the moving shock front faster than  $U_{\text{in}}(t - D_f(t))$ .

We introduce a new coordinate  $z$  defined as

$$z = \begin{cases} \frac{l(t) - x}{u}, & x \in [0, l(t)], \\ \frac{x - l(t)}{u}, & x \in [l(t), L], \end{cases} \quad (36)$$

and new variables  $\tilde{\varrho}_f(z, t)$  and  $\tilde{\varrho}_c(z, t)$  defined in  $z$ -coordinate. The transformations between  $\tilde{\rho}_f(x, t)$ ,  $\tilde{\rho}_c(x, t)$  and  $\tilde{\varrho}(z, t)$ ,  $\tilde{\varrho}_c(z, t)$  are given by

$$\tilde{\varrho}_f(z, t) = \tilde{\rho}_f(l(t) - uz, t), \quad z \in [0, D_f(t)], \quad (37)$$

$$\tilde{\varrho}_c(z, t) = \tilde{\rho}_c(l(t) + uz, t), \quad z \in [0, D_c(t)], \quad (38)$$

and the associated inverse transformations of (37) and (38) are given by

$$\tilde{\rho}_f(x, t) = \tilde{\varrho}_f\left(\frac{l(t) - x}{u}, t\right), \quad x \in [0, l(t)], \quad (39)$$

$$\tilde{\rho}_c(x, t) = \tilde{\varrho}_c\left(\frac{x - l(t)}{u}, t\right), \quad x \in [l(t), L]. \quad (40)$$

Using (37) and (38), the original system (25)-(29) is rewritten in the new  $z$ -coordinate as

$$\partial_t \tilde{\varrho}_f(z, t) = \left(1 - \frac{\dot{l}(t)}{u}\right) \partial_z \tilde{\varrho}_f(z, t), \quad z \in [0, D_f(t)], \quad (41)$$

$$\partial_t \tilde{\varrho}_c(z, t) = \left(1 + \frac{\dot{l}(t)}{u}\right) \partial_z \tilde{\varrho}_c(z, t), \quad z \in [0, D_c(t)], \quad (42)$$

$$\tilde{\varrho}_f(D_f(t), t) = U_{\text{in}}(t), \quad (43)$$

$$\tilde{\varrho}_c(D_c(t), t) = U_{\text{out}}(t), \quad (44)$$

with the ODE given by

$$\dot{X}(t) = -b(\tilde{\varrho}_f(0, t) + \tilde{\varrho}_c(0, t)). \quad (45)$$

##### B. Predictor-based backstepping transformation

We consider the following backstepping transformation, motivated by the predictor-based transformation for delay representation  $\varrho_f(z, t)$  and  $\varrho_c(z, t)$  defined in (41)-(44),

$$w_f(z, t) = \tilde{\varrho}_f(z, t) - K_f \left( X(t) - b \int_0^z \tilde{\varrho}_f(\xi, t) d\xi - b \int_0^{\min\{D_c(t), z\}} \tilde{\varrho}_c(\xi, t) d\xi \right), \quad z \in [0, D_f(t)], \quad (46)$$

$$w_c(z, t) = \tilde{\varrho}_c(z, t) - K_c \left( X(t) - b \int_0^z \tilde{\varrho}_c(\xi, t) d\xi - b \int_0^{\min\{D_f(t), z\}} \tilde{\varrho}_f(\xi, t) d\xi \right), \quad z \in [0, D_c(t)]. \quad (47)$$

where  $K_f, K_c > 0$  are positive constant gain kernels.

The above transformation in the original PDE state variables  $\rho_f(x, t)$  for  $x \in [0, l(t)]$  and  $\rho_c(x, t)$  for  $x \in [l(t), L]$ , is given by

$$w_f(x, t) = \tilde{\rho}_f(x, t) - K_f \left( X(t) - \frac{b}{u} \int_x^{l(t)} \tilde{\rho}_f(\xi, t) d\xi - \frac{b}{u} \int_{l(t)}^{\min\{L, 2l(t) - x\}} \tilde{\rho}_c(\xi, t) d\xi \right), \quad x \in [0, l(t)], \quad (48)$$

$$w_c(x, t) = \tilde{\rho}_c(x, t) - K_c \left( X(t) - \frac{b}{u} \int_{l(t)}^x \tilde{\rho}_c(\xi, t) d\xi - \frac{b}{u} \int_{\max\{0, 2l(t) - x\}}^{l(t)} \tilde{\rho}_f(\xi, t) d\xi \right), \quad x \in [l(t), L]. \quad (49)$$

- For the case  $D_f(t) \leq D_c(t)$ , it follows that  $l(t) \in [0, \frac{L}{2}]$  and the following holds

$$x \in [0, l(t)] \implies \min\{L, 2l(t) - x\} = 2l(t) - x. \quad (50)$$

- For the case  $D_f(t) \geq D_c(t)$ , it follows that  $l(t) \in [\frac{L}{2}, L]$ , the following holds

$$x \in [l(t), L] \implies \max\{0, 2l(t) - x\} = 2l(t) - x. \quad (51)$$

Later on, two pairs of state feedback controllers are obtained respectively for  $l(t) \in [0, \frac{L}{2}]$  and  $l(t) \in [\frac{L}{2}, L]$ . The inverse transformation of (48),(49) is given by

$$\begin{aligned} \tilde{\rho}_f(x, t) = & w_f(x, t) + K_f \left( X(t) - \frac{b}{u} \int_x^{l(t)} w_f(\xi, t) d\xi \right. \\ & \left. - \frac{b}{u} \int_{l(t)}^{\min\{L, 2l(t)-x\}} w_c(\xi, t) d\xi \right), \quad x \in [0, l(t)], \end{aligned} \quad (52)$$

$$\begin{aligned} \tilde{\rho}_c(x, t) = & w_c(x, t) + K_c \left( X(t) - \frac{b}{u} \int_{l(t)}^x w_c(\xi, t) d\xi \right. \\ & \left. - \frac{b}{u} \int_{\max\{0, 2l(t)-x\}}^{l(t)} w_f(\xi, t) d\xi \right), \quad x \in [l(t), L]. \end{aligned} \quad (53)$$

Let us denote the above transformations as

$$\tilde{\rho}_f = \mathcal{T}_f[w_f, w_c], \quad (54)$$

$$\tilde{\rho}_c = \mathcal{T}_c[w_f, w_c]. \quad (55)$$

At the moving interface, we have

$$w_f(l(t), t) = \tilde{\rho}_f(l(t), t) - K_f X(t), \quad (56)$$

$$w_c(l(t), t) = \tilde{\rho}_c(l(t), t) - K_c X(t). \quad (57)$$

Taking temporal and spatial derivative on both sides of (48),(49) and substituting into the PDE-ODE original system (25)-(29), we obtain target system by  $w_f(x, t)$  and  $w_c(x, t)$ ,

$$\partial_t w_f + u \partial_x w_f = \frac{K_f b}{u} \dot{l}(t)(g(t) + 2\epsilon_c(x, t)), \quad x \in [0, l(t)], \quad (58)$$

$$\partial_t w_c - u \partial_x w_c = \frac{K_c b}{u} \dot{l}(t)(g(t) - 2\epsilon_f(x, t)), \quad x \in [l(t), L], \quad (59)$$

$$w_f(0, t) = 0, \quad (60)$$

$$w_c(L, t) = 0, \quad (61)$$

$$\dot{X}(t) = -aX(t) - b(w_c(l(t), t) + w_f(l(t), t)), \quad (62)$$

where the constant coefficient  $a = b(K_f + K_c) > 0$  is obtained by substituting (56),(57) into (29), given  $b, K_f, K_c > 0$ . The time-varying term  $g(t)$  is defined as

$$g(t) = (K_f - K_c)X(t) + w_f(l(t), t) - w_c(l(t), t), \quad (63)$$

and the space and time-varying terms  $\epsilon_c(x, t)$  and  $\epsilon_f(x, t)$  are given by

$$\begin{aligned} \epsilon_c(x, t) = & \tilde{\rho}_c(2l(t) - x, t) \\ = & \mathcal{T}_c[w_f, w_c](2l(t) - x, t), \end{aligned} \quad (64)$$

$$\begin{aligned} \epsilon_f(x, t) = & \tilde{\rho}_f(2l(t) - x, t) \\ = & \mathcal{T}_f[w_f, w_c](2l(t) - x, t). \end{aligned} \quad (65)$$

We assume that densities outside freeway segment  $[0, L]$  are at steady states, therefore  $\tilde{\rho}_c(2l(t)-x, t) = 0$  when  $2l(t)-x > L$ ,

and  $\tilde{\rho}_f(2l(t) - x, t) = 0$  when  $2l(t) - x < 0$ . Hence, the followings hold for  $\epsilon_f(x, t)$  and  $\epsilon_c(x, t)$ ,

$$\begin{cases} \epsilon_f(x, t) = 0, & l(t) \in [0, L/2] \text{ and } x \in [2l(t), L], \\ \epsilon_c(x, t) = 0, & l(t) \in [L/2, L] \text{ and } x \in [0, 2l(t) - L]. \end{cases} \quad (66)$$

Otherwise,  $\epsilon_f(x, t)$  and  $\epsilon_c(x, t)$  are given by expressions in (64) and (65). The bilateral state feedback boundary actuations for inlet and outlet of the segment are derived from (48),(49) and (60),(61) as

$$\begin{aligned} U_{\text{in}}(t) = & K_f \left( X(t) - \frac{b}{u} \int_0^{l(t)} \tilde{\rho}_f(\xi, t) d\xi \right. \\ & \left. - \frac{b}{u} \int_{l(t)}^{\min\{L, 2l(t)\}} \tilde{\rho}_c(\xi, t) d\xi \right), \end{aligned} \quad (67)$$

$$\begin{aligned} U_{\text{out}}(t) = & K_c \left( X(t) - \frac{b}{u} \int_{l(t)}^L \tilde{\rho}_c(\xi, t) d\xi \right. \\ & \left. - \frac{b}{u} \int_{\max\{0, 2l(t)-L\}}^{l(t)} \tilde{\rho}_f(\xi, t) d\xi \right). \end{aligned} \quad (68)$$

We obtain two pairs of controller designs for  $l(t) \in [0, \frac{L}{2}]$  and  $l(t) \in [\frac{L}{2}, L]$ , respectively. When  $l(t) \in [0, \frac{L}{2}]$ , it holds true that  $\min\{L, 2l(t)\} = 2l(t)$ ,  $\max\{0, 2l(t) - L\} = 0$  and when  $l(t) \in [\frac{L}{2}, L]$  one gets  $\min\{L, 2l(t)\} = L$ ,  $\max\{0, 2l(t) - x\} = 2l(t)$ .

In addition, when  $l(t) = \frac{L}{2}$ , controller integral forms become identical for  $l(t) \in [0, \frac{L}{2}]$  and  $l(t) \in [\frac{L}{2}, L]$ :

$$U_{\text{in}}(t) = K_f \left( X(t) - \frac{b}{u} \int_0^{\frac{L}{2}} \tilde{\rho}_f(\xi, t) d\xi - \frac{b}{u} \int_{\frac{L}{2}}^L \tilde{\rho}_c(\xi, t) d\xi \right), \quad (69)$$

$$U_{\text{out}}(t) = K_c \left( X(t) - \frac{b}{u} \int_0^{\frac{L}{2}} \tilde{\rho}_f(\xi, t) d\xi - \frac{b}{u} \int_{\frac{L}{2}}^L \tilde{\rho}_c(\xi, t) d\xi \right). \quad (70)$$

It is remarkable that the bilateral control input smoothly switches between the above control laws when the moving interface position passes through the middle of the freeway segment.

Due to the invertibility of the transformation in (48),(49), stability of the target system  $(w_c(x, t), w_f(x, t), X(t))$  and stability the plant  $(\tilde{\rho}_f(x, t), \tilde{\rho}_c(x, t), X(t))$  are equivalent. In the next section, we apply Lyapunov analysis to prove the stability of the target system. Define the  $H^1$ -norm  $\|f(\cdot, t)\|_{H^1_{[a,b]}}$  as

$$\|f(\cdot, t)\|_{H^1_{[a,b]}} = \left( \int_a^b f^2(x, t) + f_x^2(x, t) dx \right)^{1/2}. \quad (71)$$

We now state the main result of the paper.

*Theorem 1:* Consider a closed-loop system consisting of the PDE-ODE system (11)-(13) and the bilateral full-state feedback control laws for inlet and outlet (67),(68). For any system reference  $(\rho_f^*, \rho_c^*, l^*)$  which satisfies conditions (19),(20) and (22), and for any given  $L > 0$ , there exist  $c > 0$ ,  $\gamma > 0$ ,  $\zeta > 0$  such that if the initial conditions of

the system  $(\rho_f(x, 0), \rho_c(x, 0), l(0))$  satisfy  $Z(0) < \zeta$ , local exponential stability of the closed-loop system with bilateral control laws holds  $\forall t \in [0, \infty)$ , namely,

$$Z(t) \leq ce^{-\gamma t} Z(0), \quad (72)$$

where  $Z(t)$  is defined as

$$Z(t) = \|\rho_f(x, t) - \rho_f^*\|_{H^1_{[0, l(t)]}} + \|\rho_c(x, t) - \rho_c^*\|_{H^1_{[l(t), L]}} + |l(t) - l^*|^2, \quad (73)$$

and condition (14) is satisfied for model validity.

## V. PROOF OF THEOREM 1

In the proof, the local stability of the closed-loop system in the  $H^1$  sense is shown with Lyapunov analysis and the following condition of model validity (14) is guaranteed by our control design. The proof of Theorem 1 is established through following steps: we firstly prove the local stability of the target system (58)-(62) for a given time interval  $\forall t \in [0, t^*)$  under the assumption that condition (14) is satisfied. Then we prove that with initial conditions of states variables bounded, the local exponential stability of the above target system holds for  $\forall t \in [0, \infty)$  with the assumption removed. This is achieved by comparison principle and contradiction proof in Lemma 3. In the end, the stability analysis of the target system leads to stability of the original PDE-ODE system in (11)-(13).

Let us define the Lyapunov functional

$$V(t) = V_1(t) + V_2(t) + \lambda V_3(t) + \lambda V_4(t) + V_5(t), \quad (74)$$

where  $\lambda > 0$  with the component Lyapunov functions

$$V_1(t) = \int_0^{l(t)} e^{-x} w_f^2(x, t) dx, \quad (75)$$

$$V_2(t) = \int_{l(t)}^L e^{x-L} w_c^2(x, t) dx, \quad (76)$$

$$V_3(t) = \int_0^{l(t)} e^{-x} \partial_x w_f^2(x, t) dx, \quad (77)$$

$$V_4(t) = \int_{l(t)}^L e^{x-L} \partial_x w_c^2(x, t) dx, \quad (78)$$

$$V_5(t) = X(t)^2. \quad (79)$$

*Lemma 1:* Assume  $\exists t^* > 0$  such that the condition in (14) is satisfied, then there exists  $\sigma > 0$  such that the following holds  $\forall t \in [0, t^*)$ ,

$$\dot{V}(t) \leq -\sigma V + \tau V^{3/2}. \quad (80)$$

**Proof:** Taking time derivative of the Lyapunov function (74) along the solution of the target system (58)-(62), we have

$$\begin{aligned} \dot{V}_1(t) = & -u \int_0^{l(t)} e^{-x} w_f^2(x, t) dx - (u - \dot{l}(t)) e^{-l(t)} w_f^2(l(t), t) \\ & + \frac{2K_f b}{u} \dot{l}(t) g(t) \int_0^{l(t)} e^{-x} w_f(x, t) dx \\ & + \frac{4K_f b}{u} \dot{l}(t) \int_0^{l(t)} e^{-x} \epsilon_c(x, t) w_f(x, t) dx, \end{aligned} \quad (81)$$

$$\begin{aligned} \dot{V}_2(t) = & -u \int_{l(t)}^L e^{x-L} w_c^2(x, t) dx - (u + \dot{l}(t)) e^{l(t)-L} w_c^2(l(t), t) \\ & + \frac{2K_c b}{u} \dot{l}(t) g(t) \int_{l(t)}^L e^{x-L} w_c(x, t) dx \\ & - \frac{4K_c b}{u} \dot{l}(t) \int_{l(t)}^L e^{x-L} \epsilon_f(x, t) w_c(x, t) dx, \end{aligned} \quad (82)$$

$$\begin{aligned} \dot{V}_3(t) = & -u \int_0^{l(t)} e^{-x} \partial_x w_f^2(x, t) dx \\ & - (u - \dot{l}(t)) e^{-l(t)} \partial_x w_f^2(l(t), t) + u \partial_x w_f^2(0, t) \\ & + \frac{4K_f b}{u} \dot{l}(t) \int_0^{l(t)} e^{-x} \partial_x \epsilon_c(x, t) \partial_x w_f(x, t) dx, \end{aligned} \quad (83)$$

$$\begin{aligned} \dot{V}_4(t) = & -u \int_{l(t)}^L e^{x-L} \partial_x w_c^2(x, t) dx \\ & - (u + \dot{l}(t)) e^{l(t)-L} \partial_x w_c^2(l(t), t) + u \partial_x w_c^2(L, t) \\ & - \frac{4K_c b}{u} \dot{l}(t) \int_{l(t)}^L e^{x-L} \partial_x \epsilon_f(x, t) \partial_x w_c(x, t) dx, \end{aligned} \quad (84)$$

$$\dot{V}_5(t) = -aX(t)^2 - b(w_c(l(t), t) + w_f(l(t), t)) X(t). \quad (85)$$

By Agmon's inequality, the followings hold

$$w_f^2(l(t), t) \leq \|w_f\|_\infty^2 \leq 4 \|\partial_x w_f\|_2^2 = 4V_3, \quad (86)$$

$$w_c^2(l(t), t) \leq \|w_c\|_\infty^2 \leq 4 \|\partial_x w_c\|_2^2 = 4V_4. \quad (87)$$

Plugging the above inequalities into the ODE (62) yields that there exists  $\delta > 0$  such that

$$|\dot{l}(t)| < a\sqrt{V_5} + b(\sqrt{V_3} + \sqrt{V_4}) < \delta\sqrt{V}. \quad (88)$$

Using Young's inequality, Cauchy-Schwarz inequality for (63) and (86),(87), we have

$$g(t)^2 \leq \mu_1 V_3 + \mu_2 V_4 + \mu_3 V_5, \quad (89)$$

where  $\mu_j > 0, j = 1, 2, 3$ . By definition of  $\epsilon_c(x, t)$  in (64), there exist  $\eta_k > 0, k = 1, 2, 4$  such that

$$\int_0^{l(t)} \epsilon_c^2(x, t) dx \leq \eta_1 V_1 + \eta_2 V_2 + \eta_4 V_4. \quad (90)$$

It follows that

$$\begin{aligned} \dot{V}_1(t) \leq & -uV_1 + |\dot{l}(t)| w_f^2(l(t), t) \\ & + \frac{2K_f b}{u} |\dot{l}(t)| \left( g^2(t) + \int_0^{l(t)} w_f^2(x, t) dx \right) \\ & + \frac{4K_f b}{u} |\dot{l}(t)| \left( \int_0^{l(t)} \epsilon_c^2(x, t) dx + \int_0^{l(t)} w_f^2(x, t) dx \right), \end{aligned} \quad (91)$$

Plugging (86) and (88)-(90) into the above inequality, there exists  $\kappa_1 > 0$  such that

$$\dot{V}_1(t) \leq -uV_1 + \kappa_1 V^{3/2}, \quad (92)$$

Taking total time derivative of boundary condition (60) yields,

$$\partial_x w_f(0, t) = \frac{K_f b}{u^2} \dot{l}(t) (g(t) + 2\epsilon_c(0, t)), \quad (93)$$

Given definition of  $\epsilon_c(x, t)$  in (64), there exist  $\nu_0, \nu > 0$  such that

$$\epsilon_c(0, t) < \nu_0 V, \quad (94)$$

$$\int_0^{l(t)} \partial_x \epsilon_c^2(x, t) < \nu V. \quad (95)$$

Using Young's inequality and plugging (89) and (94) into (93), we obtain that there exists  $\theta > 0$  such that

$$\partial_x w_f^2(0, t) \leq \frac{K_c b}{u^2} |\dot{l}(t)| (g^2(t) + 4\epsilon_c^2(0, t)) < \theta V^{3/2}, \quad (96)$$

Plugging (86), (88), (95) and (96) into (83), we obtain that there exists  $\kappa_3 > 0$  such that

$$\dot{V}_3(t) \leq -uV_3 + \kappa_3 V^{3/2}, \quad (97)$$

In the same fashion, we could obtain that there exist  $\kappa_2, \kappa_4 > 0$  such that

$$\dot{V}_2(t) \leq -uV_2 + \kappa_2 V^{3/2}, \quad (98)$$

$$\dot{V}_4(t) \leq -uV_4 + \kappa_4 V^{3/2}, \quad (99)$$

For the last Lyapunov component, the following holds

$$\dot{V}_5(t) \leq -aV_5 + \frac{4b}{a}V_3 + \frac{4b}{a}V_4. \quad (100)$$

Using inequalities (92) and (97)-(100) into (74), it follows that

$$\begin{aligned} \dot{V}(t) &\leq -uV_1 - uV_2 - \left( \lambda u - \frac{4b}{a} \right) V_3 \\ &\quad - \left( \lambda u - \frac{4b}{a} \right) V_4 - aV_5 + \tau V^{3/2}. \end{aligned} \quad (101)$$

where  $\tau = \kappa_1 + \kappa_2 + \lambda\kappa_3 + \lambda\kappa_4 > 0$ . We choose  $\lambda$  such that

$$\lambda > \frac{4b}{au}, \quad (102)$$

thus it holds that for  $\sigma = \min \left\{ u - \frac{4b}{\lambda a}, a \right\}$ ,

$$\dot{V}(t) \leq -\sigma V + \tau V^{3/2}. \quad (103)$$

□

*Lemma 2:* According to (80), for any  $\sigma_0$  such that  $0 < \sigma_0 < \sigma$ , there exists  $\delta_0 > 0$  such that for any  $V(0) < \delta_0$ ,

$$\tau |V^{3/2}| < (\sigma - \sigma_0)V \quad (104)$$

and,

$$\dot{V}(t) \leq -\sigma_0 V. \quad (105)$$

By comparison principle, the exponential stability is satisfied that  $\forall t \in [0, t^*]$ ,

$$V(t) \leq V(0)e^{-\sigma_0 t} < \delta_0. \quad (106)$$

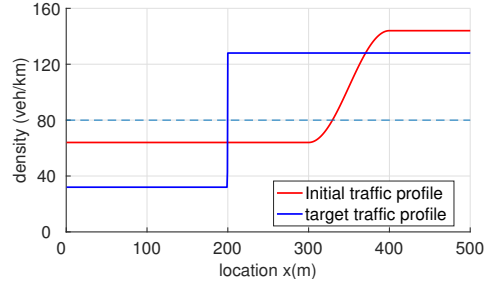


Fig. 3. Traffic density profiles for initial condition with a soft shockwave and target system on freeway

*Lemma 3:* If the initial conditions of the target system  $(w_f(x, 0), w_c(x, 0), X(0))$  satisfy the following

$$V(0) \leq \min\{\delta_0, \delta_1\}, \quad (107)$$

where the positive constant  $\delta_1$  is defined as

$$\delta_1 = \min \{ (L - l^*)^2, l^{*2} \}. \quad (108)$$

Then Lyapunov functional inequality (105) and condition (14) hold for  $t \in [0, \infty)$ .

*Proof:* We assume that there exists  $t^* > 0$  such that condition (14) is satisfied for  $t \in [0, t^*)$  but is violated at  $t = t^*$ . Given (107) and by comparison principle, the following inequality holds

$$V(t^*) \leq V(0) < \delta_1. \quad (109)$$

According to the definition of  $V(t)$  in (74), we obtain that

$$X^2(t^*) < V(t^*). \quad (110)$$

Combining (108) and (109), we have

$$X^2(t^*) < \delta_1 = \min \{ (L - l^*)^2, l^{*2} \}. \quad (111)$$

Since  $l(t^*) = X(t^*) + l^*$  and  $0 < l^* < L$ , we obtain from (111) that

$$0 < l(t^*) < L. \quad (112)$$

We conclude that (112) contradicts the assumption that (14) is violated at  $t = t^*$ . Therefore, the condition (14) is guaranteed for  $t \in [0, \infty)$  when the initial condition  $V(0)$  satisfies (107). This completes the proof Lemma 3.

Due to invertibility of the transformation in (48),(49), we conclude that the system (25)-(29) with control laws (67),(68) is locally exponentially stable in the  $H^1$  norm, which completes the proof of Theorem 1. □

## VI. SIMULATION

We simulate proposed control design considering a moving traffic shockwave in a 500-meter freeway segment. The initial condition of the traffic profile and the desirable target traffic profile  $\rho_f^* = 32$  vehs/km,  $\rho_c^* = 128$  vehs/km,  $l^* = 200$  m,  $\rho_{\text{jump}} = 80$  vehs/km are shown in Fig. 3, where the position of the shockwave front is initially located at 330-meter and the final setpoint location is at 200-meter. The initial position of the shockwave front is in the right-half plane of

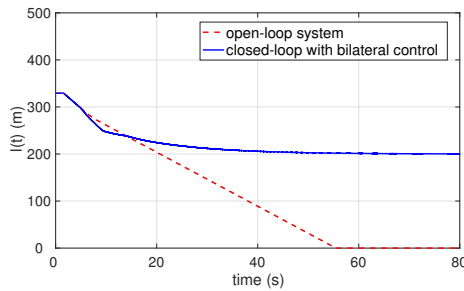


Fig. 4. Evolution of the moving interface position  $l(t)$  for open-loop system and for closed-loop system with bilateral boundary control

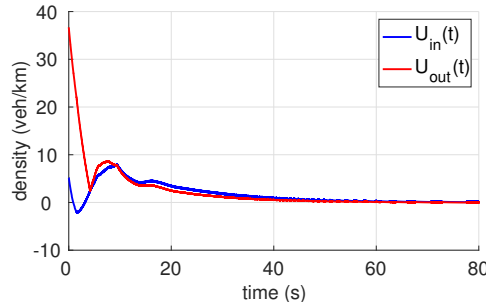


Fig. 5. Evolution of bilateral control inputs over time

the segment while its final position is located at the left-half plane of the segment. The control objective is to regulate PDE states and ODE state from the initial profile to the reference profile.

In Fig. 4, after around 40s, the moving interface position stops at the setpoint location  $l = 200$  m with bilateral control while in open-loop system it propagates upstream and travels out of the freeway segment before 1 min. In Fig. 5, one can observe that the bilateral control signals, the control inputs also converge to zeros after around 40s.

## VII. CONCLUSION

This paper addresses boundary feedback control problem of moving shockwave in congested traffic described by an PDE-ODE system. To stabilize the coupled system to a desired setpoint, we use predictor-based backstepping method to transform the state-dependent PDE-ODE coupled system to a target system, where the PDE state-dependent input delays to ODE are compensated by the bilateral boundary control inputs to PDEs. Actuators of traffic densities at both boundaries are considered. The local exponential stability in  $H^1$  norm is achieved and the model validity is guaranteed with the control designs. For future work, general theoretical results on multiple PDEs state-dependent input delays cascading to a nonlinear ODE is of authors' interest.

## REFERENCES

[1] G. Bastin, J. M. Coron, A. Hayat, & P. Shang. "Boundary feedback stabilization of hydraulic jumps". *IFAC Journal of Systems and Control*, 100026, 2019.

[2] N. Bekiaris-Liberis, & M. Krstic. "Robustness of nonlinear predictor feedback laws to time-and state-dependent delay perturbations". *Automatica*, 49(6), 1576-1590, 2013.

[3] N. Bekiaris-Liberis, & M. Krstic. "Compensation of state-dependent input delay for nonlinear systems". *IEEE Transactions on Automatic Control*, 58(2), 275-289, 2013.

[4] N. Bekiaris-Liberis, & M. Krstic. "Predictor-feedback stabilization of multi-input nonlinear systems". *IEEE Transactions on Automatic Control*, 62(2):516531, 2017.

[5] F. Belletti, M. Huo, X. Litrico, & A. M. Bayen. "Prediction of traffic convective instability with spectral analysis of the AwRascleZhang model," *Physics Letters A*, 379(38), 2319-2330, 2015.

[6] R. Borsche, R. M. Colombo, & M. Garavello. "Mixed systems: ODEs balance laws". *Journal of Differential equations*, 252(3), 2311-2338, 2012.

[7] M. Buisson-Fenet, S. Koga, & M. Krstic. "Control of Piston Position in Inviscid Gas by Bilateral Boundary Actuation." In *2018 IEEE Conference on Decision and Control (CDC)* (pp. 5622-5627). IEEE, 2018.

[8] X. Cai, & M. Krstic. "Nonlinear control under wave actuator dynamics with timeand statedependent moving boundary". *International Journal of Robust and Nonlinear Control*, 25(2), 222-251, 2015.

[9] M. L. Delle Monache, & P. Goatin. "Scalar conservation laws with moving constraints arising in traffic flow modeling: an existence result". *Journal of Differential equations*, 257(11), 4015-4029, 2014.

[10] M. Diagne, N. Bekiaris-Liberis, & M. Krstic. "Time and State Dependent Input Delay Compensated BangBang Control of a Screw Extruder for 3D Printing," *International Journal of Robust and Nonlinear Control*, 27(17), 3727-3757, 2017.

[11] M. Diagne, N. Bekiaris-Liberis, A. Otto, & M. Krstic. "Control of transport PDE/nonlinear ODE cascades with state-dependent propagation speed". *IEEE Transactions on Automatic Control*, 62(12), 6278-6293, 2017.

[12] I. Karafyllis, N. Bekiaris-Liberis, & M. Papageorgiou. "Feedback Control of Nonlinear Hyperbolic PDE Systems Inspired by Traffic Flow Models". *IEEE Transactions on Automatic Control*, 2018.

[13] Koga, S., & Krstic, M. "Arctic sea ice temperature profile estimation via backstepping observer design". In *2017 IEEE Conference on Control Technology and Applications (CCTA)*, (pp. 1722-1727), 2017.

[14] S. Koga, D. Straub, M. Diagne, & M. Krstic. "Thermodynamic Modeling and Control of Screw Extruder for 3D Printing". In *2018 Annual American Control Conference (ACC)*, (pp. 2551-2556), 2018.

[15] C. Lattanzio, A. Maurizi, & B. Piccoli. "Moving shockwaves in car traffic flow: a PDE-ODE coupled model". *SIAM Journal on Mathematical Analysis*, 43(1), 50-67, 2011.

[16] M. Treiber, & A. Kesting. "Traffic flow dynamics: data, models and simulation". *Physics Today*, 67(3), 54, 2014.

[17] D. Tsubakino, M. Krstic, & T. R. Oliveira, "Exact predictor feedbacks for multi-input LTI systems with distinct input delays". *Automatica*, 71, 143-150, 2016.

[18] S. Villa, P. Goatin, & C. Chalons. "Moving bottlenecks for the Aw-Rascle-Zhang traffic flow model". *Discrete and Continuous Dynamical Systems-Series B*, 22(10), 3921-3952, 2016.

[19] J. Wang, S. Koga, Y. Pi, & M. Krstic. "Axial Vibration Suppression in a Partial Differential Equation Model of Ascending Mining Cable Elevator". *Journal of Dynamic Systems, Measurement, and Control*, 140(11), 111003, 2018.

[20] H. Yu, and M. Krstic, "Traffic congestion control for Aw-Rascle-Zhang model," *Automatica*, vol.100, pp.38-51, 2019.

[21] H. Yu, and M. Krstic. "Varying Speed Limit Control of Aw-Rascle-Zhang Traffic Model," In *2018 21st IEEE International Conference on Intelligent Transportation Systems (ITSC)*, (pp. 1846-1851). IEEE, 2018.

[22] H. Yu, and M. Krstic. "Traffic congestion control on Aw-Rascle-Zhang model: Full-state feedback," In *2018 Annual American Control Conference (ACC)*, (pp. 943-948). IEEE, 2018.

[23] H. Yu, and M. Krstic. "Adaptive Output Feedback for Aw-Rascle-Zhang Traffic Model in Congested Regime," In *2018 Annual American Control Conference (ACC)*, (pp. 3281-3286). IEEE.

[24] H. Yu, S. Koga, & M. Krstic. "Stabilization of Traffic Flow With a Leading Autonomous Vehicle," In *ASME 2018 Dynamic Systems and Control Conference*, (pp. V002T22A006-V002T22A006). American Society of Mechanical Engineers, 2018.

[25] L. Zhang, C. Prieur, & J. Qiao. "PI boundary control of linear hyperbolic balance laws with stabilization of ARZ traffic flow models". *Systems & Control Letters*, 123, 85-91, 2019.

[26] L. Zhang, C. Prieur, & J. Qiao. "Local Exponential Stabilization of Semi-Linear Hyperbolic Systems by Means of a Boundary Feedback Control". *IEEE Control Systems Letters*, 2(1), 55-60, 2018.